Inorganic Chemistry

Article

pubs.acs.org/IC

Nona-Coordinated Chiral Eu(III) Complexes with Stereoselective Ligand−Ligand Noncovalent Interactions for Enhanced Circularly Polarized Luminescence

Takashi Harada,*[,†] Hiroyuki Tsumatori,[‡] Katsura Nishiyama,[†] Junpei Yuasa,[‡] Yasuchika Hasegawa,[§] and Tsuyoshi Kawai*[,‡]

[†]Faculty of Education, Shimane University, Matsue, Shimane 690-8504, Japan

[‡]Graduate School of Materials Science, Nara Institute of Science and Technology, 8916-5 Takayama-Cho, Ikoma, Nara 630-0192, Japan

[§]Divisions of Materials Chemistry, Graduate School of Engineering, Hokkaido University, North-13 West-8, Kita-Ku, Sapporo, Hokkaido 060-8628, Japan

Supporting Information

ABSTRACT: Circularly polarized luminescence (CPL) of chiral Eu(III) complexes with nona- and octa-coordinated structures, [Eu(*R*/*S*-iPr-Pybox)(*D*-facam)$_3$] (**1-*R*/1-*S***; *R*/*S*-iPr-Pybox, 2,6-bis(4*R*/4*S*-isopropyl-2-oxazolin-2-yl)pyridine; *D*-facam, 3-trifluoroacetyl-*d*-camphor), [Eu(*S*,*S*-Me-Ph-Pybox)(*D*-facam)$_3$] (**2-*SS***; *S*,*S*-Me-Ph-Pybox, 2,6-bis(4*S*-methyl-5*S*-phenyl-2-oxazolin-2-yl)pyridine), and [Eu(Phen)(*D*-facam)$_3$] (**3**; Phen, 1,10-phenanthroline) are reported, and their structural features are discussed on the basis of X-ray crystallographic analyses. These chiral Eu(III) complexes showed relatively intense photoluminescence due to their $^5D_0 \rightarrow {}^7F_1$ (magnetic-dipole) and $^5D_0 \rightarrow {}^7F_2$ (electric-dipole) transition. The dissymmetry factors of CPL (g_{CPL}) at the former band of **1-*R*** and **1-*S*** were as large as −1.0 and −0.8, respectively, while the g_{CPL} of **3** at the $^5D_0 \rightarrow {}^7F_1$ transition was relatively small (g_{CPL} = −0.46). X-ray crystallographic data indicated specific ligand−ligand hydrogen bonding in these compounds which was expected to stabilize their chiral structures even in solution phase. CPL properties of **1-*R*** and **1-*S*** were discussed in terms of transition nature of lanthanide luminescence.

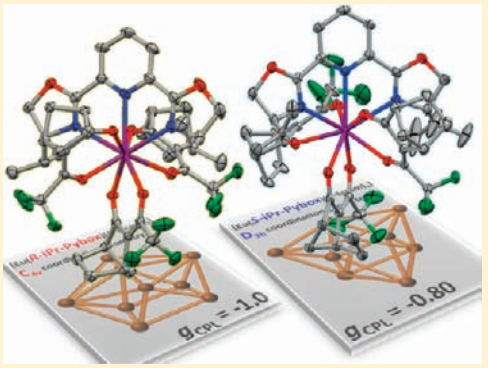

INTRODUCTION

Coordination compounds with chiral organic ligands are of great interest to chemists in the fields of asymmetric catalysis[1] and chiroptical materials.[2] Structural dissymmetry around the metal center primarily controls their asymmetric response for chemical reagents and for circularly polarized light. Design of coordination chirality for highly enantioselective chemical reactions requires fine-tuning and precise control of ligand−metal geometry and ligand−ligand interaction. Meanwhile, some chiral organic and inorganic compounds dissymmetrically emit circularly polarized luminescence (CPL),[3,4] which are expected for future active materials in display and sensing applications.[5] Among various luminescent chiral coordination compounds, lanthanide(III) complexes with chiral organic ligands exhibit characteristic CPL properties[4] due to electric-dipole[6] and magnetic-dipole transitions.[7] Since some lanthanide(III), Ln(III), ions, such as Eu(III), Sm(III), or Tb(III) have various coordination numbers and coordination geometries, as exemplified in Figure 1;[8] enantioselective control for their coordination geometry is still a challenging subject.[4a] In some Ln(III) compounds with enantiopure organic ligands, diastereomeric isomers with opposite inner-sphere chirality have been observed.[9] Since such pseudoracemization on the

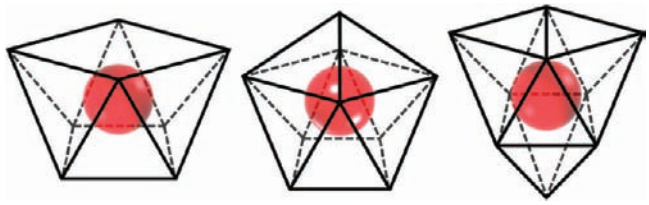

Figure 1. Coordination geometry around the Eu(III) center with square antiprism (left), capped square antiprism (center), and tricapped trigonal prism (right).

coordination geometry should depress the CPL activity,[4d,f] chirality inductions by means of multidentate helicate ligands and stereoselective ligand−ligand noncovalent interactions have been proposed for providing the chemical species which is chiroptically pure in solution phase.[4b,e,9−11] Difficulty for predicting coordination geometry and effective enantio-purity in solution phase motivated us to explore further CPL active

Received: November 16, 2011
Published: June 5, 2012

   dx.doi.org/10.1021/ic202467f | *Inorg. Chem.* 2012, 51, 6476−6485

Ln(III) complexes considering control for ligand−ligand interaction.

We herein study novel chiral Eu(III) complexes with an anionic chiral ligand, 3-trifluoroacetyl-*d*-camphor (*D*-facam), and chiral tridentate ligands, bis-4*R*-(4-isopropyl-oxalozin-yl)pyridine (*R*-iPr-Pybox), bis-4*S*-(4-isopropyl-oxalozin-yl)-pyridine (*S*-iPr-Pybox), and bis-*4S,4S*-(4-methyl-5-phenyl-oxazolin-yl)pyridine (*S,S*-Me-Ph-Pybox), such as [Eu(*R*-iPr-Pybox)(*D*-facam)$_3$], **1-*R***, [Eu(*S*-iPr-Pybox)(*D*-facam)$_3$], **1-*S***, and [Eu(*S,S*-Me-Ph-Pybox)(*D*-facam)$_3$], **2-*SS*** (chemical structures are illustrated in Figure 2). The Pybox ligands have been

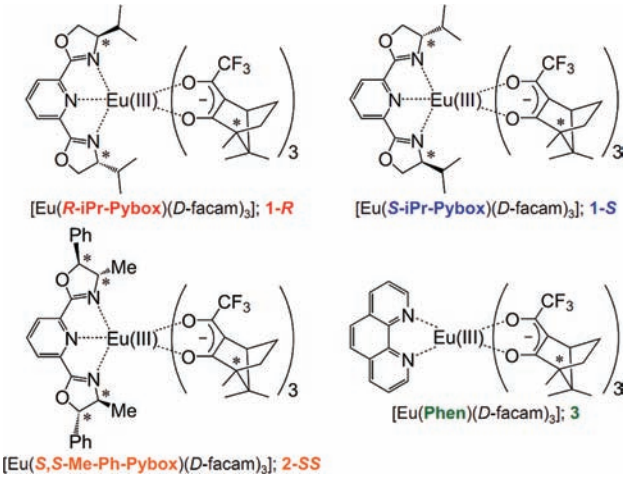

Figure 2. Chemical structures of chiral Eu(III) complexes.

reported to selectively stabilize an asymmetric arrangement of cocoordinating achiral bidentate ligands around a metal center through stereoselective ligand−ligand interactions, which provided relatively large CPL activity.[11,12] Meanwhile, [Eu(*D*-facam)$_3$] has been previously reported to show intense CPL activity although its emission intensity is rather weak.[13] Inserted Pybox ligands are expected to encapsulate the Eu(III) center from surrounding solvents and to suppress vibrational decay of excited state. Moreover, specific stereoselective interaction between two types of ligands, Pybox and *D*-facam, are also expected. In our previous study, introduction of prochiral organic ligands into [Eu(*D*-facam)$_3$] resulted in pseudoracemization on arrangement of *D*-facam ligands and diastereomeric coordination isomers with suppressed CPL activity.[9c] Considering the large CPL dissymmetry of an anionic complex [Eu(*D*-facam)$_4$]$^-$,[14] we introduced Pybox ligands as a chiral tridentate ligand to [Eu(*D*-facam)$_3$]. A chiral octa-coordinated Eu(III) complex with N-bidentate 1,10-phenanthroline (Phen), [Eu(Phen)(*D*-facam)$_3$] (**3**), was also prepared for comparison. We report on steady state emission, emission decay, and CPL properties of these chiral Eu(III) compounds and compare them with single crystal structures.

EXPERIMENTAL SECTION

Apparatus. ^{1}H NMR was obtained with a JEOL AL-300 spectrometer. Electrospray ionization mass spectrometry (ESI-MS) was recorded with a JEOL JMS-700 mass spectrometer. Infrared spectra were recorded with a JASCO FT/IR-4200 spectrometer. Elemental analyses were performed with a Perkin-Elmer, 2400 II.

Materials. 2,6-Bis(4*R*-isopropyl-2-oxazolin-2-yl)pyridine (*R*-iPr-Pybox) and 2,6-bis(4*S*-isopropyl-2-oxazolin-2-yl)pyridine (*S*-iPr-Pybox) were purchased from Tokyo Chemical Industry Co., Ltd. 1,10-Phenanthroline monohydrate (Phen) was purchased from Nacalai Tesque, Inc. Tris(3-trifluoroacetyl-*d*-camphorato)europium-(III) ([Eu(*D*-facam)$_3$]: purity >97%) and 2,6-bis(4*S*-methyl-5*S*-phenyl-2-oxazolin-2-yl)pyridine (*S,S*-Me-Ph-Pybox) were purchased from Aldrich Chemical Co. Inc. All other organic compounds were reagent grade and used as received.

Preparation of Tris (3-Trifluoroacetyl-*d*-camphorato)-europium(III) 2,6-bis(4*R*-isopropyl-2-oxazolin-2-yl)pyridine ([Eu(*R*-iPr-Pybox)(*D*-facam)$_3$], 1-*R*). [Eu(*D*-facam)$_3$] (0.43 g, 0.46 mmol) and *R*-iPr-Pybox (0.14 g, 0.46 mmol) were dissolved in methanol (50 mL) and refluxed under stirring for 12 h. The reaction solution was left at rest, and pale yellow crystals were obtained by filtration. The crystals were washed with *n*-hexane and dried in vacuo. Yield: 46%. ESI-MS (Positive): 946.288 ([M-(*D*-facam)]$^+$) *m*/*z*. ^{1}H NMR ($CDCl_3$, 300 MHz, 298 K) δ: 12.6−11.0 (br), 9.0−7.6 (br), 6.8−5.8 (br), 1.89 (br), −1.0 to −2.2 (br), −2.8 to −3.4 (br), −3.8 to −5.0 (br) ppm. FT-IR (ATR): 3010−2810 (w, br, C−H), 1651 (s, sh, C═O), 1585 (w), 1522 (s), 1483 (w), 1441 (w), 1371 (m), 1329 (m, CF_3), 1294 (w, CF_3), 1267 (s, CF_3), 1225 (s, CF_3), 1200 (m, CF_3), 1182 (s, CF_3), 1122 (s, CF_3), 1111 (m), 1082 (m), 1051 (m), 1009 (s), 972 (m), 922 (w), 891 (w), 850 (w), 829 (w), 802 (m), 746 (m), 714 (w), 683 (m), 644 (w) cm^{-1}. Anal. Found: C, 52.98%; H, 5.24%; N, 3.66%. Calcd. for $EuC_{53}H_{65}N_3O_8F_9$: C, 53.27%; H, 5.48%; N, 3.52%.

Preparation of Tris (3-Trifluoroacetyl-*d*-camphorato)-europium(III) 2,6-bis(4*S*-isopropyl-2-oxazolin-2-yl)pyridine ([Eu(*S*-iPr-Pybox)(*D*-facam)$_3$], 1-*S*). **1-*S*** was prepared in the same way as given in the synthesis of **1-*R***, using *S*-iPr-Pybox (0.14 g, 0.46 mmol) instead of *R*-iPr-Pybox in methanol. The reaction solution was left at rest. The pale yellow crystals were washed with *n*-hexane and dried in vacuo. Yield: 34%. ESI-MS (Positive): 946.288 ([M-(*D*-facam)]$^+$) *m*/*z*. ^{1}H NMR ($CDCl_3$, 300 MHz, 298 K) δ: 9.2−7.8 (br), 6.6−5.6 (br), 2.04 (s, br), −0.4 to −2.0 (br), −3.0 to −4.0 (br) ppm. FT-IR (ATR): 3010−2810 (w, br, C−H), 1651 (s, sh, C═O), 1585 (w), 1522 (s), 1481 (w), 1439 (w), 1369 (m), 1327 (m, CF_3), 1294 (w, CF_3), 1267 (s, CF_3), 1225 (s, CF_3), 1200 (m, CF_3), 1182 (s, CF_3), 1109 (s, CF_3), 1080 (w), 1049 (w), 1005 (s), 970 (m), 922 (w), 891 (w), 850 (w), 829 (w), 802 (m), 746 (m), 714 (w), 683 (m), 644 (w) cm^{-1}. Anal. Found: C, 53.12%; H, 5.34%; N, 3.59%. Calcd. for $EuC_{53}H_{65}N_3O_8F_9$: C, 53.27%; H, 5.48%; N, 3.52%.

Preparation of Tris (3-Trifluoroacetyl-*d*-camphorato)-europium(III) 2,6-bis(4*S*-methyl-5*S*-phenyl-2-oxazolin-2-yl)-pyridine ([Eu(*S,S*-Me-Ph-Pybox)(*D*-facam)$_3$], 2-*SS*). [Eu(*D*-facam)$_3$] (0.26 g, 0.29 mmol) and *S,S*-Me-Ph-Pybox (0.12 g, 0.29 mmol) were added in the flask. Acetonitrile (20 mL) and methanol (20 mL) were added in the flask in rotation. The reaction solution was refluxed with stirring for 12 h. The reaction solution was left at rest, and the pale yellow crystals were obtained by the recrystallization. The crystals were washed with *n*-hexane and dried in vacuo. Yield: 73%. ESI-MS (Positive): 1042.288 ([M-(*D*-facam)]$^+$) *m*/*z*. ^{1}H NMR ($CDCl_3$, 300 MHz, 298K) δ: 12.0−11.2 (s, br), 9.03 (s, br), 8.5−7.8 (br), 7.7−7.4 (d, br), 2.6−2.0 (br), 1.5−0.5 (br), −1.39 (br), −1.78 (br), −2.61 (br), −3.36 (br), −4.64 (br) ppm. FT-IR (ATR): 3050−2800 (br, w, C−H), 1658 (sh, s, C═O), 1581 (w), 1527 (s), 1427 (m), 1377 (w), 1331 (w), 1265 (s, CF_3), 1223 (s, CF_3), 1184 (s, CF_3), 1126 (s, CF_3), 1080 (w), 1049 (w), 1011 (w), 949 (m), 837 (w), 802 (m), 748 (m), 690 (m), 644 (w) cm^{-1}. Anal. Found: C, 56.09%; H, 4.84%; N, 3.41%. Calcd. for $EuC_{61}H_{65}N_3O_8F_9{\cdot}0.5H_2O$: C, 56.35%; H, 5.12%; N, 3.23%.

Preparation of Tris (3-Trifluoroacetyl-*d*-camphorato)-europium(III) 1,10-phenanthroline ([Eu(Phen)(*D*-facam)$_3$], 3). **3** was prepared in the same way as given in the synthesis of **1-*R***, using 1,10-phenanthroline monohydrate (0.045 g, 0.26 mmol) instead of *R*-iPr-Pybox and [Eu(*D*-facam)$_3$] (0.21 g, 0.23 mmol). The reaction solution was left at rest. The obtained pale yellow crystals were washed with *n*-hexane and dried in vacuo. Yield: 72%. ESI-MS (Positive): 825.177 ([M-(*D*-facam)]$^+$) *m*/*z*. ^{1}H NMR ($CDCl_3$, 300 MHz, 298K) δ: 10.49 (d, Aromatic, 2H), 10.23 (s, Ar, 2H), 7.97 (d, Ar, 2H), 4.92 (s, Ar, 2H), 2.56 (s, 3H), 2.06 (s, 9H), 1.23 (t, 3H), 0.52 (t, 3H), −0.09 (s, 9H), −0.71 (s, 3H), −0.83 (s, 9H), −1.62 (t, 3H) ppm. FT-IR (ATR): 3025−2800 (br, w, C−H), 1647 (sh, s, C═O), 1535 (m),

dx.doi.org/10.1021/ic202467f | *Inorg. Chem.* 2012, 51, 6476−6485

Table 1. Crystal Data, Data Collection, and Structural Refinement Data of Eu(III) Complexes

	1-*R*	1-*S*	2-*SS*	3
chemical formula	$C_{53}H_{65}EuN_3O_8F_9$	$C_{53}H_{65}EuN_3O_8F_9$	$C_{61}H_{65}EuN_3O_8F_9$	$C_{48}H_{50}EuN_2O_6F_9$
formula weight	1195.06	1195.06	1291.15	1073.88
crystal system	orthorhombic	monoclinic	monoclinic	monoclinic
space group	P_{212121} (#19)	P_{21} (#4)	P_{21} (#4)	P_{21} (#4)
a/Å	20.0635(4)	21.3203(4)	10.0931(3)	16.3485(3)
b/Å	23.0466(4)	23.1025(4)	13.4287(3)	12.6514(2)
c/Å	36.3584(7)	22.3797(4)	22.2764(5)	22.9499(4)
α/deg	90.0(0)	90.0(0)	90.0(0)	90.0(0)
β/deg	90.0(0)	90.2315(7)	95.8361(7)	99.7100(7)
γ/deg	90.0(0)	90.0(0)	90.0(0)	90.0(0)
V/Å^3	16811.9(5)	11023.1(3)	3003.6(1)	4678.77(15)
Z^a	12	8	2	4
T/K	103 ± 1	103 ± 1	123 ± 1	103 ± 1
μ (Mo Kα)/cm^{-1}	11.989	12.190	11.245	14.230
measured reflections	139303	91160	29534	46776
unique reflections	30686	40132	13605	21166
R_1	0.0255	0.0229	0.0313	0.0230
$R(R_w)$	0.0632	0.0570	0.0746	0.0556
goodness of fitting	1.039	1.124	1.175	1.078

^{a}Z values of P_{212121} and P_{21} space groups are theoretically 4 and 2, respectively. The departures between the observed and the theoretical Z values for **1-*R***, **1-*S***, and **3** are due to the observed multistructures in the minimum unit of these Eu(III) complexes.

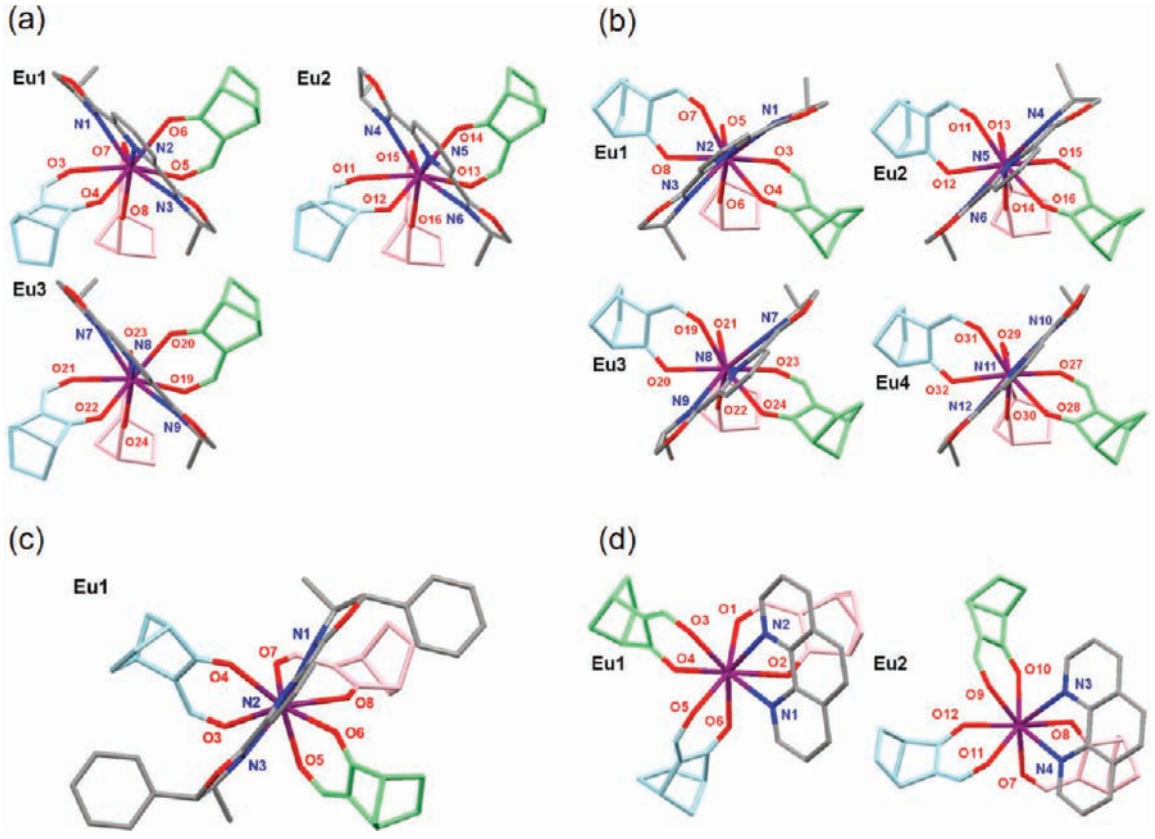

Figure 3. X-ray structures of (a) **1-*R***, (b) **1-*S***, (c) **2-*SS***, and (d) **3**. Purple atoms; Eu, red; O, blue; N, gray, light blue, light green; C. Hydrogen atoms are not illustrated.

1423 (m), 1327 (m), 1294 (w), 1265 (s, CF_3), 1222 (s, CF_3), 1198 (s, CF_3), 1180 (s, CF_3), 1124 (s, CF_3), 1107 (m), 1078 (m), 1049 (m), 920 (w), 847 (m), 802 (m), 729 (m), 681 (w), 642 (w) cm^{-1}. Anal. Found: C, 53.69%; H, 4.57%; N, 2.61%. Calcd. for $EuC_{48}H_{50}N_2O_6F_9$: C, 53.69%; H, 4.69%; N, 2.61%.

Optical Measurements. UV−vis, circular dichroism (CD), and the emission spectra were detected at room temperature with JASCO V-550, JASCO J-725, and JASCO FP-6500 spectrometers, respectively. The obtained emission spectra were corrected for detector sensitivity and lamp intensity variations. For measurements of emission and CPL spectra, the Eu(III) complexes were dissolved in acetone-d_6 and acetonitrile-d_3 and maintained in a quartz cell with optical path length 10 mm, while degassed with N_2 bubbling. The emission quantum yields excited at 465 nm were estimated by comparing the integrated

dx.doi.org/10.1021/ic202467f | *Inorg. Chem.* 2012, 51, 6476−6485

emission intensity and absorbance at the excitation wavelength with those of [Eu(BIPHEPO)(*D*-facam)$_3$] solution (dissolved in acetone-d_6, 0.01 M, Φ_{em} = 3.1%) as a reference.[9c] In the emission lifetime measurements, samples were excited by a N_2 laser (Usho KEC-160, wavelength; 337 nm, pulse width; 600 ps, repitation; 10 Hz). Time evolution of emission spectra was recorded using a streak camera (Hamamatsu, C4780). The CPL spectra measurements were performed using a handmade system,[3f] where excitation wavelength was 375 nm.

X-ray Crystallography. X-ray diffraction images were collected with a Rigaku RAXIS RAPID (3 kW) system with an imaging plate detector and a graphite monochromated Mo Kα radiation at 103 ± 1 K. Nonhydrogen atoms were refined anisotropically. Hydrogen atoms were placed in calculated positions (C−H; 0.95 Å) and not refined. All calculations were performed with Rigaku CrystalStructure 3.8.1 and CrystalStructure 3.8.2 software. The analyses using CF_3 conformations in Eu(III) complexes were carried out according to the literature.[15]

RESULTS AND DISCUSSION

Coordination Structures. Single crystal X-ray analyses of **1-*R***, **1-*S***, **2-*SS***, and **3** were successfully performed. Crystallographic data of Eu(III) complexes are listed in Table 1. Chemical structures of **1-*R***, **1-*S***, **2-*SS***, and **3** in the crystalline lattice are illustrated in Figure 3.

Three nona-coordinated structures of **1-*R***, four nona-coordinated structures of **1-*S***, and two octa-coordinated structures of **3** were observed in these crystals, while **2-*SS*** showed a single nona-coordinated structure. The isomers of **1-*R*** and **1-*S*** revealed similar coordination structures as shown in Figure 3a,b. To understand structural features of these complexes, we tried to assign the alignment of inner sphere atoms to the typical nona-coordination structures by means of least shape measure parameter, *S*.[21] *S* parameter, defined with eq i, is evaluated by comparing the observed coordination structure with assumed ideal structures such as CSAP or TTP,[16]

$$S(\delta, \theta) = \min\left[\sqrt{\left(\frac{1}{m}\right)\sum_{i=1}^{m}(\delta_i - \theta_i)^2}\right] \quad \text{(i)}$$

where m, δ_i, and θ_i are the number of all the possible edges (e.g., m = 18 for SAP), an observed dihedral angle between planes along the ith edge, and a dihedral angle for the ideal structure, respectively. Minimization of *S* values is carried out regarding all possible orientations of the observed atomic alignment relative to the ideal coordination structure.[20] Detailed procedure and data for evaluating these *S* values are also provided in the Appendix in Supporting Information.[16,17] Calculated *S* values of **1-*R***, **1-*S***, **2-*SS***, and **3** are listed in Table 2. Assumption of CSAP for the Eu1 site in **1-*R*** afforded a smaller *S* value than that for TTP, suggesting CSAP as a better assignment. However, the difference in *S* parameters between those for CSAP and TTP is only 0.24, which indicated substantial distortion in the practical structures with respect to these ideal structures. Similarly, all assignments for **1-*R***, **1-*S***, and **2-*SS*** provided rather small differences in the *S* values for CSAP and TTP. In the case of compound **3**, both structures revealed the smallest *S* values for SAP, which were about one-half or less of those for BTP and TD. This significant difference in *S* values indicates better adequacy for the assignment to SAP.

Coordination geometry of **1-*R*** and **1-*S*** are illustrated in Figure 4, regarding their structural assignment for CSAP and TTP. Although chirality of the coordination structures given in Figures 3 and 4 is not easily understood, the three isomers of **1-*R*** in Figure 3 seem to have quite similar geometry. Topologically, these isomers can interconvert to the others without cleavage of the coordination bonding. Such isomerization is possible to proceed without large energy uptake or activation energy. Otherwise phrased, these isomers of **1-*R*** are able to behave effectively as a same isomer in solution phase while they are fixed in the crystal lattice. These isomers of **1-*R*** obviously have similar structural chirality as shown in Figure 3. These isomers are thus expected to provide cooperative effects on both CD and CPL in solution phase even if they exist as distinct chemical species in solution phase. Also, **1-*S*** shows similar pseudostereoisomerism in the crystal state. The inner sphere coordination geometry of the Eu1 site of ***1-R*** is similar to that of the Eu1 site of ***1-S***, though they look like a mirror image of each other. The apparent structural chirality in respect to the iPr-Pybox ligands seems to be primarily determined by the absolute configuration around the isopropyl groups. We then turned to the coordination geometry of *D*-facam ligands for comparison of geometries of ***1-R*** and ***1-S***, as illustrated in Figure 5.

Table 2. Shape Measure Estimation (*S* values) of 1-*R*, 1-*S*, and 2-*SS* for Nona-Coordinated CSAP, $S(C_{4v})$ and TTP, and $S(D_{3h})$, and *S* values of 3 for Octa-Coordinated SAP, $S(D_{4d})$, Trigonal Dodecahedron, $S(D_{2d})$, and Bicapped Trigonal Prism, $S(C_{2v})$, and Their Suitable Coordination Geometries

complex	site	$S(C_{4v})$	$S(D_{3h})$		geometry
1-*R*	Eu1	6.15	6.39		CSAP
	Eu2	7.98	5.89		TTP
	Eu3	6.50	8.19		CSAP
1-*S*	Eu1	8.34	10.05		CSAP
	Eu2	9.86	9.36		TTP
	Eu3	9.97	6.68		TTP
	Eu4	8.91	6.85		TTP
2-*SS*		6.97	6.01		TTP
complex	site	$S(D_{4d})$	$S(D_{2d})$	$S(C_{2v})$	geometry
3	Eu1	6.22	14.61	11.72	SAP
	Eu2	5.50	14.15	11.57	SAP

The β-diketonato planes of *D*-facam are illustrated in light-green and dark-green for the front and the back faces whose definition is also illustrated in Figure 5, respectively. Pybox ligands are omitted here for brevity.[11] We here denote three *D*-facam ligands in each coordination structure as *D*-facam-1, *D*-facam-2, and *D*-facam-3 according to the number of oxygen atoms. From the given fixed viewpoint, all three *D*-facam ligands in both **1-*R*** and ***1-S*** show their front plane. The dihedral angle between *D*-facam-1 and *D*-facam-2 for **1-*R*** was 86 degrees and was close with that between *D*-facam-1 and *D*-facam-3 for **1-*S***, 87.4 degrees. These results indicated structural similarity of **1-*R*** and ***1-S*** in respect to the *D*-facam ligands. On the other hand, as illustrated in Figure 6, the two isomers of SAP structures in compound **3** can be assigned to two enantiomeric structures. That is, compound **3** forms pseudoracemic crystals composed of an equivalent amount of Eu1 and Eu2 isomers of opposite chirality. Bond lengths and angles between Eu(III) ions and nitrogen and oxygen atoms in **1-*R***, **1-*S***, **2-*SS***, and **3** are summarized in Tables S1 and S2 in Supporting Information. These parameters are comparable to those in previously reported Eu(III) complexes.[9c,11,14]

We then studied ligand−ligand interactions for investigating the origins of the difference in coordination geometries of these compounds. Figure 8 shows noncovalent interactions between

dx.doi.org/10.1021/ic202467f | Inorg. Chem. 2012, 51, 6476−6485

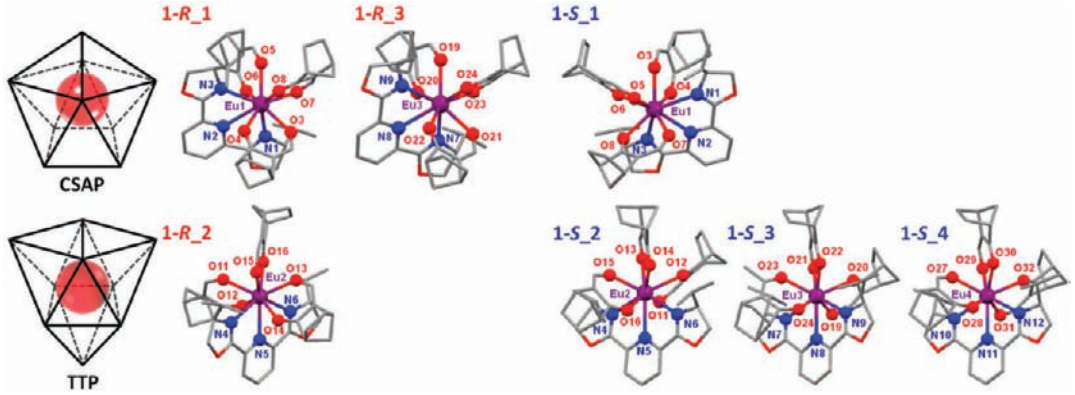

Figure 4. Assignment of coordination structures of Eu1, Eu2, and Eu3 sites in **1-*R*** and Eu1, Eu2, Eu3, and Eu4 sites in **1-*S*** giving CSAP and TTP geometries with minimized *S* values. Some atoms are omitted for clarity. Atomic color, purple; Eu, red; O, blue; N, gray; C.

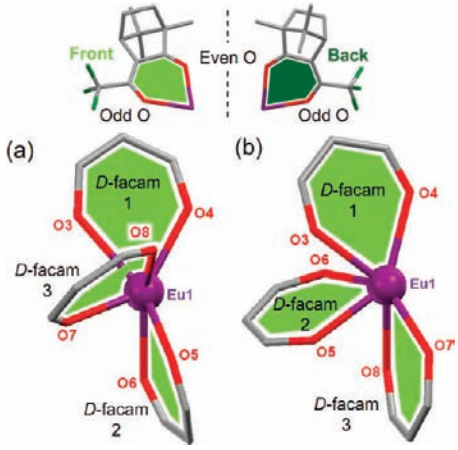

Figure 5. *β*-diketonato planes of *D*-facam ligands in (a) **1-*R*** and (b) **1-*S***.

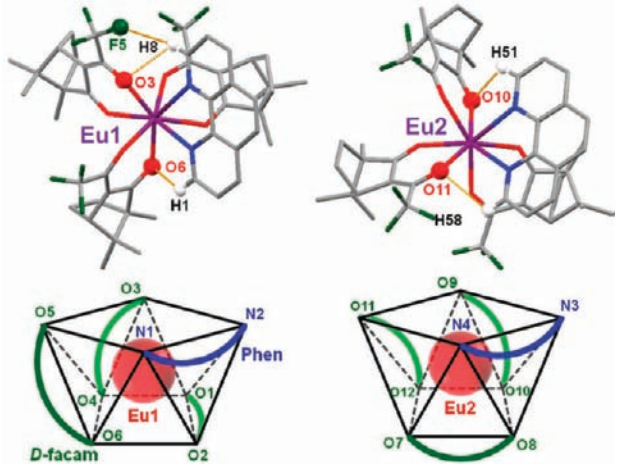

Figure 6. Ligand–ligand interactions (upper) and coordination geometry of *D*-facam ligands (lower) in **3**.

Pybox and *D*-facam in **1-*R***, **1-*S***, and **2-*SS***, which are identified in the crystal structures. Hydrogen atoms in isopropyl groups in **1-*R*** and **1-*S*** are close to oxygen atoms in the *D*-facam ligands with distance shorter than the sum of van der Waals radii of these atoms (2.7 Å), for example, H1–O7, 2.59 Å; H2–O6, 2.67 Å; H8–O3, 2.68 Å; H20–O4, 2.62 Å for Eu1 site of **1-*R***; H3–O5, 2.63 Å; H8–O3, 2.68 Å; H16–O8, 2.55 Å; H17–O6, 2.60 Å for Eu1 site of **1-*S***. They indicated ligand–ligand C–H···O hydrogen bonding.[9c,11,18] As illustrated in Figure 7, **1-*R*** and **1-*S*** exhibited 4-fold hydrogen bonding in each complex. Similar C–H···O hydrogen bonding was observed in both oxazoline rings of each iPr-Pybox ligand in **1-*R*** and **1-*S***, while one oxazoline ring in **2-*SS*** contributed to the dual hydrogen bonding (H20–O3, 2.68 Å; H21–O5, 2.60 Å). Figure 6 also indicates similar ligand–ligand interactions in compound **3**.[11,18] Two ligand–ligand interactions are observed which are also possible to stabilize both isomers in the crystal phase. There are *D*-facam ligands free from the ligand–ligand interaction. Their coordination geometry might not be well controlled; since chiral induction usually requires stereocontrol through three or more anchoring points. The more sterically crowded nona-coordinated compounds **1-*R*** and **1-*S*** provided specific four-point ligand–ligand interactions in their crystalline states.

We also observed specific intermolecular interactions in the Eu(III) complexes, as shown in Figures S1–S4, Supporting Information. In contrast to the intramolecular–interligand interactions, C–H···F and C–H···O with the oxygen on oxazoline rings were mainly observed in each complex. In addition, complex **3** showed intermolecular *π*–*π* interactions between two Phen rings as shown in Figure S4, Supporting Information. We suggest that intramolecular ligand–ligand interactions could hold chiral coordination structures loosely, although the interligand interactions could yield unexpected coordination isomers like complex **3**.

UV–Vis and Circular Dichroism Spectra. UV–vis and CD spectra of the Eu(III) complexes are shown in Figure 8.

Absorption maxima at 310 nm observed for these compounds are assigned to the *π*–*π** transition of *D*-facam ligands.[9c] Molar absorption coefficients, *ε* at 310 nm are 2.9 × 10^4 $M^{-1}cm^{-1}$ for **1-*R***, **1-*S***, and **2-*SS***, and 3.0 × 10^4 $M^{-1}cm^{-1}$ for **3**, respectively. **1-*R***, **1-*S***, and **2-*SS*** also show broad absorption bands corresponding to the Pybox ligands in the wavelength range between 200 and 300 nm (see Figure S5 in Supporting Information). Compound **3** revealed distinct absorption bands at 265 nm as $\varepsilon = 3.6 \times 10^4$ $M^{-1}cm^{-1}$ and at 230 nm as $\varepsilon = 5.0 \times 10^4$ $M^{-1}cm^{-1}$, which stemmed from the Phen ligand. **1-*R***, **1-*S***, and **3** showed positive CD bands around 310 nm. These positive CD bands are similar to those of previous Eu(III) complexes containing *D*-facam ligands.[9c] In contrast, **2-*SS*** exhibited a split CD band with an interception at 313 nm. Considering the exciton-coupling between *D*-facam ligands as the origin of these CD bands,[14,19,20] the characteristic CD profile of **2-*SS*** suggests its specific arrangement of *D*-facam

dx.doi.org/10.1021/ic202467f | *Inorg. Chem.* 2012, 51, 6476–6485

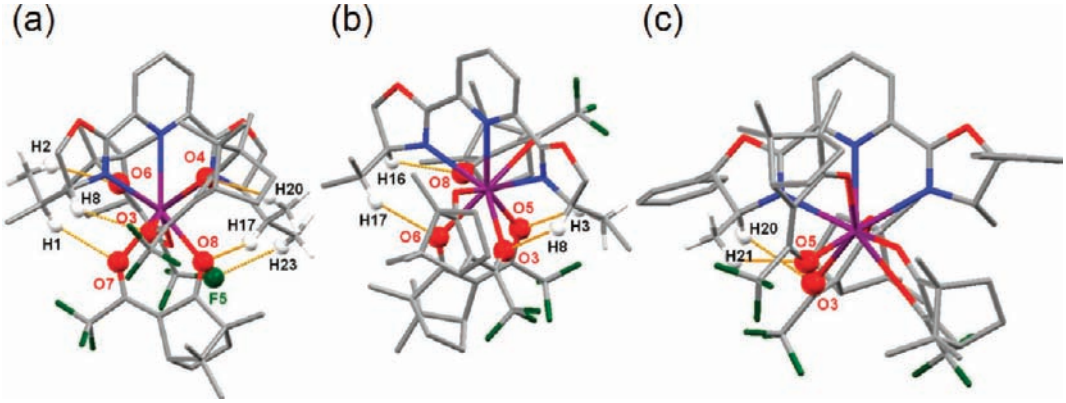

Figure 7. Ligand–ligand interactions of (a) **1-*R***, Eu1 site, (b) **1-*S***, Eu1 site, and (c) **2-*SS***. Purple atoms; Eu, red; O, blue; N, green; F, gray; C. Some atoms are omitted for clarity.

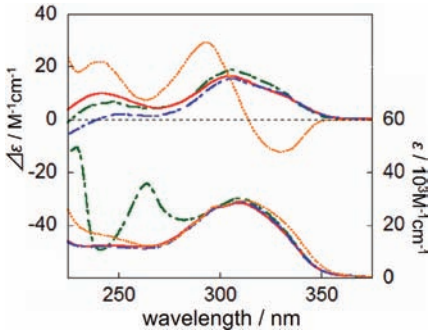

Figure 8. UV–vis (lower) and CD (upper) spectra of **1-*R*** (red line, 9.5 μM), **1-*S*** (blue, 8.5 μM), **2-*SS*** (orange, 7.6 μM), and **3** (green, 8.9 μM). Solvents used were methanol for **1-*R***, **1-*S***, and **3** and THF for **2-*SS*** (**2-*SS*** is insoluble in methanol).

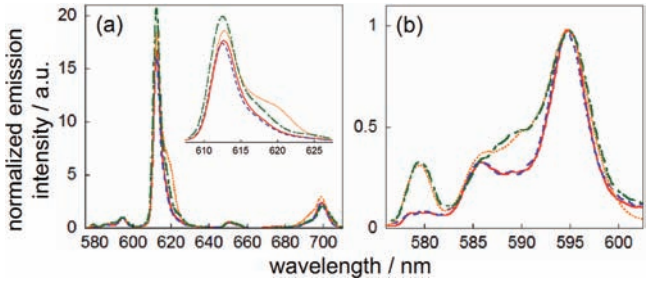

Figure 9. (a) Normalized emission spectra of the Eu(III) complexes, **1-*R*** (red), **1-*S*** (blue), **2-*SS*** (orange), and **3** (green). Inset: expansion of domains corresponding to the $^5D_0 \rightarrow {}^7F_2$ transition. (b) Expansion of the domains corresponds to the $^5D_0 \rightarrow {}^7F_0$ and the $^5D_0 \rightarrow {}^7F_1$ transitions. Note that these spectra were normalized at 594 nm. Solvents used were acetone-d_6 (1.0 mM).

ligands, which differs from those of **1-*R*** and **1-*S*** in solution phase as observed in their crystal structures illustrated in Figures 3–7. In the shorter wavelength range, the CD signals are in the order of **2-*SS*** > **1-*R*** > **3** > **1-*S***, which are in accordance with the cooperative CD effect of *D*-facam and N-coordinated ligands free in solution (see Figure S5, Supporting Information). Magnitude of optical dissymmetry is evaluated with g_{CD} value, which is defined as follows:[2a–g]

$$g_{CD} = \frac{\Delta\varepsilon}{\varepsilon} = \frac{\varepsilon_L - \varepsilon_R}{\frac{1}{2}(\varepsilon_L + \varepsilon_R)} \qquad \text{(ii)}$$

where ε and $\Delta\varepsilon$ express the molar absorption coefficient and the molar absorption coefficient toward left- and right-circularly polarized light, ε_L and ε_R, respectively. The g_{CD} values of **2-*SS*** are -5.6×10^{-4} at 330 nm, 1.2×10^{-3} at 290 nm, and 1.3×10^{-3} at 240 nm, respectively. On the other hand, the g_{CD} values at 310 nm for **1-*R***, **1-*S***, and **3** are found to be 5.5×10^{-4}.

Luminescent Properties. Figure 9 shows normalized emission spectra of Eu(III) complexes dissolved in acetone-d_6. Five emission bands of the Eu(III) complexes are observed at about 580, 595, 612, 650, and 700 nm, which are assigned to the 4*f*–4*f* transitions, $^5D_0 \rightarrow {}^7F_J$ with J = 0, 1, 2, 3, and 4, respectively.[9c,21] These emission spectra were normalized with respect to the magnetic-dipole $^5D_0 \rightarrow {}^7F_1$ transition which is less sensitive to the coordination geometry.[22] The predominant electric-dipole transition band at 612 nm corresponds to the $^5D_0 \rightarrow {}^7F_2$ transition which becomes partially allowed with a crystal field of noncentrosymmetry.[6,16,22] Shoulder bands in the $^5D_0 \rightarrow {}^7F_2$ transition are observed at 620 nm for **2-*SS*** and at 618 nm for **3** as shown in the inset, which are ascribed to the crystal field splitting[6,17,18] and to different coordination fields around the Eu(III) center. The emission profile of **2-*SS*** suggests that the coordination geometry of **2-*SS*** is specific compared with other nona-coordinated **1-*R*** and **1-*S***. The similar emission profiles of **1-*R*** and **1-*S*** were also obtained in acetonitrile-d_3 (see Figure S6 and Table S3 in Supporting Information). It is worth noting that there is no marked concentration dependence in the emission profiles of **1-*R*** and **1-*S*** in concentration range between 1.0 mM and 10 μM as shown in Figure S7, Supporting Information. The binding constants between the ligands and the Eu(III) centers seem to be large enough in this concentration range, though it is not sufficient enough to provide the information for deducing the binding-dissociation nature as reported in previous literature[4b,e,5c,23] using pyridyl diamide ligands.

In order to evaluate the emission probability of the electric-dipole transition, relative integrated intensities of the $^5D_0 \rightarrow {}^7F_2$ transition band with respect to the $^5D_0 \rightarrow {}^7F_1$ transition band, A_{rel}, values were evaluated as listed in Table 3. A_{rel} of the Eu(III) complexes have been reported to be dependent mainly on probability of electric-dipole transition due to the asymmetric coordination geometry.[6,24] Emission quantum yield (Φ_{em}) and emission lifetime (τ_{em}) are also summarized in Table 3 with radiative and nonradiative rate constants (k_r and k_{nr}, respectively) which are simply evaluated as $k_r = \Phi_{em}/\tau_{em}$ and $k_{nr} = (1-\Phi_{em})/\tau_{em}$. **1-*R*** and **1-*S*** showed single exponential emission decay, while dual exponential emission decay was

dx.doi.org/10.1021/ic202467f | *Inorg. Chem.* 2012, 51, 6476–6485

Table 3. Summary of Emission Properties of Eu(III) Complexes

complex	Φ_{em}[a]/%	$\tau_{em}/\mu s$	k_r/s^{-1}	k_{nr}/s^{-1}	A_{rel}[b]
1-*R*	0.89 ± 0.09	260 ± 11	34	3.8×10^3	15
1-*S*	0.89 ± 0.10	260 ± 13	34	3.8×10^3	16
2-*SS*	0.50 ± 0.15	15 ± 2 (94%), 240 ± 9 (6%)			16
3	0.54 ± 0.17	30 ± 3 (97%), 280 ± 18 (3%)			18

[a] Φ_{em} values in acetone-d_6 (1.0 mM) were measured by excitation at 465 nm ($^7F_0 \rightarrow {}^5D_2$, the direct excitation band of Eu(III) ion). τ_{em} values were measured by excitation at 337 nm. [b] $A_{rel} = A_{5D0\rightarrow7F2}/A_{5D0\rightarrow7F1}$, where $A_{5D0\rightarrow7F2}$ and $A_{5D0\rightarrow7F1}$ are the integrated emission intensities of the $^5D_0 \rightarrow {}^7F_2$ and $^5D_0 \rightarrow {}^7F_1$ transition bands. Note that superscripts and subscripts are not used in $A_{5D0\rightarrow7F2}$ and $A_{5D0\rightarrow7F1}$ for clarity.

observed in **2-*SS*** as in **3**. The coordination structures of **1-*R*** and **1-*S*** are regarded as efficiently stabilized to give the single emission lifetime in the solution phase. Characteristic time-dependent evolution of the emission profile was clearly observed for **2-*SS***, as shown in Figure S8, Supporting Information. These results suggest that there exists two or more emissive species in equilibrium for compounds **2-*SS*** and **3**, which have different excited state lifetimes and emission profiles. The multicomponent emission decay of compound **3** might be thus attributed to its diastereomeric isomerism. It is also possible that the longer emission lifetime of **3** is attributed to dissociation of Phen ligands because the emission lifetime of [Eu(*D*-facam)$_3$] is also found to be 280 μs (1.0 mM, in acetone-d_6) and similar to the longer one of **3**. The relatively small emission quantum yields of present Eu(III) complexes could be attributed to chemical structures of the N-coordination ligands.[2S,26] They contain highly vibronic C−H moieties on the chiral-center carbon atoms, which are the second nearest neighbors around the Eu(III) center and able to induce vibronic-coupled nonradiative decay of the excited Eu(III) center.[11,25] The *D*-facam ligands may also contribute to the enhanced nonradiative decay because of their C−H bonding.

CPL Properties. CPL spectra of the Eu(III) complexes in acetone-d_6 are shown in Figure 10.

CPL signals were clearly observed for $^5D_0 \rightarrow {}^7F_J$ bands with J = 1 at about 595 nm and those with J = 2 at about 616 nm. The CPL and emission spectra were normalized with respect to the $^5D_0 \rightarrow {}^7F_1$ and $^5D_0 \rightarrow {}^7F_2$ bands, respectively.[2a−g] These

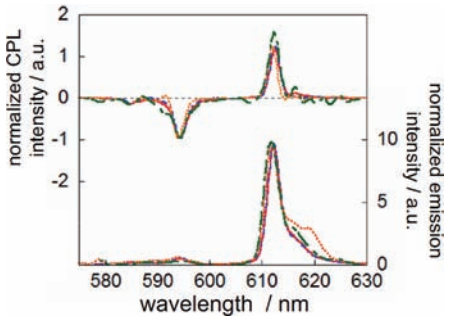

Figure 10. Normalized emission (lower) and the normalized CPL (upper) spectra of **1-*R*** (red line), **1-*S*** (blue line), **2-*SS*** (orange line), and **3** (green line). These spectra were normalized at 594 nm. Solvents used were acetone-d_6 (>3.0 mM).

Eu(III) complexes demonstrated a negative CPL signal at the $^5D_0 \rightarrow {}^7F_1$ magnetic dipole transition band and a positive CPL signal at the $^5D_0 \rightarrow {}^7F_2$ electric-dipole transition band in a similar manner. The CPL spectral sign seems to be dominantly controlled by the chirality of *D*-facam ligands if we compare the CPL profiles of **1-*R*** and **1-*S***; whereas the N-coordinated ligands provide minor effects. The CPL spectra of these Eu(III) complexes are similar to those of Eu(III) complexes with *D*-facam and P═O ligands we reported previously.[9c] On the basis of these emission and CPL spectra, g_{CPL} values were estimated using eq iii as follows,[2g]

$$g_{CPL} = \frac{\Delta I}{\frac{1}{2}I} = \frac{I_L - I_R}{\frac{1}{2}(I_L + I_R)} \qquad \text{(iii)}$$

where I, I_L, and I_R denoted the total emission intensity, left-CPL intensity, and right-CPL intensity, respectively. ΔI is $I_L - I_R$. Estimated g_{CPL} values at the $^5D_0 \rightarrow {}^7F_1$ band, g_{MD}, and at the $^5D_0 \rightarrow {}^7F_2$ band, g_{ED}, are summarized in Table 4. In all Eu(III) complexes, relatively large g_{CPL} values are obtained for the $^5D_0 \rightarrow {}^7F_1$ magnetic-dipole transition.[2c] We wish to emphasize that the g_{CPL} values obtained are significantly large as $|g_{MD}| = 0.80$ for **1-*S*** and $|g_{MD}| = 1.0$ for **1-*R*** and **2-*SS*** at the $^5D_0 \rightarrow {}^7F_1$ transition, which indicates emission of photons of left and right circular polarization with a ratio of about 25:75. These values of $|g_{MD}|$ for **1-*R***, **1-*S***, and **2-*SS*** are markedly larger than that of **3** ($|g_{MD}| = 0.46$) and also larger than that of [Eu(*D*-facam)$_3$] (in DMSO, $|g_{MD}| = 0.78$;[13] in acetone-d_6, $|g_{MD}| = 0.90$ at 594 nm, $|g_{ED}| = 0.060$ at 612 nm) according to previous literature[13] and the Supporting Information, Figure S9. The $|g_{ED}|$ values of present complexes, ca. 6.0×10^{-2}, are also notably large among those for electric-dipole transitions.

Since **1-*R*** and **1-*S*** showed the single component emission decay, we evaluated radiative rate constants for the MD and the ED transition bands, taking k_r and A_{rel} values into account. We also evaluated the difference of radiative rate constants for left- and light-CPL on both the MD and ED bands as Δk_{rMD} and Δk_{rED} ($\Delta k_{ri} = k_{ri}\, g_{CPLi}/2$). These parameters were also summarized in Table 4 with properties of typical previous Eu(III) complexes.[9c] Δk_{rMD} of each compound roughly coincided with the corresponding Δk_{rED}.[2c,g] Furthermore, these four complexes showed similar values of Δk_{rMD} and Δk_{rED} in order of magnitude, even though their coordination geometry and g_{CPL} values were substantially different. Although it is possibly just a coincidence, this tendency may suggest that the compounds with smaller k_r values show larger g_{CPL} values. In other words, suppressed k_r and k_{nr} values would be simultaneously demanded for efficient CPL compounds with large Φ_{em} and g_{CPL} values.[6a,27] Compound **3** showed relatively small $|g_{CPL}|$ values, which should be attributable to the pseudoracemization of **3** as suggested in the crystal structure analyses.

The large $|g_{CPL}|$ values of the nona-coordinated Eu(III) complexes **1-*R*** and **1-*S*** with iPr-Pybox ligands may thus originate from the arrangement of ligands by means of ligand−ligand hydrogen bonding, which might lead to higher chiroptical purity in their coordination structures in solution phase. This explanation would be supported by the observations that **1-*R*** and **1-*S*** exhibited the single-component emission lifetime and no marked concentration dependence in their emission spectra in a range between 10^{-3} and 10^{-5} M. The dissociation of Pybox ligands from these complexes produces emissive compounds [Eu(*D*-facam)$_3$] whose emission

dx.doi.org/10.1021/ic202467f | Inorg. Chem. 2012, 51, 6476−6485

Table 4. Summary of CPL Properties of Eu(III) Complexes

complex	g_{MD}[a]	k_{rMD}/s^{-1}	$\Delta k_{rMD}/s^{-1}$	g_{ED}[a]	k_{rED}/s^{-1}	$\Delta k_{rED}/s^{-1}$
1-*R*	−1.0	1.7	0.85	0.065	26	0.85
1-*S*	−0.8	1.7	0.74	0.063	27	0.85
2-*SS*	−1.0			0.076		
3	−0.46			0.020		
$[Eu((R)\text{-BINAPO})(hfa)_3]$[b]	0.030	49	0.74	−0.0028	370	0.52
$[Eu(TPPO)_2(D\text{-facam})_3]$[b]	−0.47	3.5	0.82	0.033	45	0.74

[a] g_{MD} and g_{ED} are estimated at 594 and 612 nm, respectively. Note that g_{CPL} values contain errors as much as 10%. [b] The normalized emission spectra, k_r, k_{nr}, g_{MD}, and g_{ED} values are taken from our previous reports.[9c] Other conditions are the same as those provided in Table 3.

quantum yield in acetone-d_6 is 2.0% and is comparable with those of **1-*R*** and **1-*S***. Therefore, the concentration independent emission profiles suggest that elimination equilibrium of the Pybox ligand does not occur in the present condition, which seems to be suppressed with the ligand−ligand interaction. In addition, we observed considerable emission spectral change of $[Eu(D\text{-facam})_3]$ under the titration with *R*-iPr-Pybox as illustrated in Figure S10, Supporting Information. Although the coordination of Pybox ligands would exclude the coordinated solvents or water, the emission intensities dropped along with the addition of *R*-iPr-Pybox ligands. The k_r and k_{nr} values of $[Eu(D\text{-facam})_3]$ were found to be 71 s^{-1} and 3.5×10^3 s^{-1}. We suggest that the suppressed radiation might result in the large g_{CPL} values of **1-*R***, **1-*S***, and **2-*SS***.

Under the assumption that the solution phase structures of complexes **1-*R*** and **1-*S*** are similar to those of the crystalline phase, we could expand discussion for relationship between sign of CPL and structural chirality of the coordination geometry. As observed in Figures 3 and 4, **1-*R*** and **1-*S*** have opposite chirality in respect to the arrangement of iPr-Pybox ligands, while they can be assigned to similar chirality regarding the arrangement of *D*-facam ligands as illustrated in Figure 5. The CPL activity of these complexes is dominantly controlled with the chiral *D*-facam ligands which afford the same sign of CPL signals. Electromagnetic dissymmetry around the Ln(III) center is regarded to be influenced by the chiral arrangement of primarily coordinating atoms as the point charges and by the dissymmetry in the electromagnetic susceptibility over the ligands.[2] Moreover, the anisotropic elecromagnetic susceptibility around the Eu(III) centers in the present cases may originate from the anisotropic arrangement of 6-membered rings composed of the π-conjugation system and the O/Eu(III)/O sequence in each *D*-facam/Eu(III) structure.

The relatively large $|g_{CPL}|$ value of **2-*SS*** would also be worth noting. Regarding the time evolution of emission spectra, **2-*SS*** exists as the two or more emissive isomers with different coordination geometry in the solution phase. A plausible explanation for the large $|g_{CPL}|$ and plural chiral isomers for **2-*SS*** is that every isomer emits a CPL signal with a cooperative phase. Since $|g_{CPL}|$ values of **1-*R***, **1-*S***, **2-*SS***, and **3** in acetonitrile-d_3 solution are markedly smaller than those in acetone-d_6 (see Figure S11 and Table S3 in Supporting Information), we may need to analyze coordination geometry in solution phase regarding effects of solvent and excitation circular polarization for further understanding of the CPL activity of these chiral Eu(III) complexes in solution phase.[4d]

SUMMARY AND CONCLUSIONS

Significantly large g_{CPL} values (e.g., $g_{CPL} = -1.0$) were demonstrated at the magnetic-dipole ($^5D_0 \rightarrow {}^7F_1$) transition band from the Eu(III) complexes with chiral *D*-facam and Pybox ligands. The CPL properties of chiral Eu(III) complexes were discussed considering their coordination geometry determined with the X-ray crystallographic data and photophysical properties. Pseudoracemization of coordination structure in crystal and in solution phases was regarded as an origin of suppressed CPL activity in compound **3**. In contrast, precisely controlled coordination geometry of **1-*R*** and **1-*S*** give chiroptically pure chemical species in solution and crystalline states. Specific multipoint ligand−ligand interactions are expected to suppress the pseudoracemization and lead the improved chiroptical purity in their coordination structures even in the solution phase, which is substantially effective in more sterically crowded nona-coordinated compounds with multipoint ligand−ligand atomic contacts. In addition, we note that Pybox ligands enhanced g_{CPL} of $[Eu(D\text{-facam})_3]$, as can be seen in the g_{CPL} values of **1-*R*** and **2-*SS***. The emission and CPL properties of the complexes were compared and discussed on the basis of the partially allowed transition nature of Eu(III) center and of suppressed nonradiative decay. It is worthy that we suppose a specific strategy for enhancement of CPL property based on specific electronic transition of Ln(III) luminescence. We believe that chiral Ln(III) complexes may be applied as CPL emitting molecular light source for future display, sensor, and other photofunctional applications.

ASSOCIATED CONTENT

Supporting Information

UV−vis and CD spectra of free ligands, the normalized emission and CPL spectra of the Eu(III) complexes in acetonitrile-d_3, additional ORTEP views, and shape measure estimation data of Eu(III) complexes, and the calculation model of ideal nona-coordination structures; Figures S1−S16, Tables S1−S11, and the Appendix. X-ray crystallographic data (CIF files) of **1-*R***, **1-*S***, **2-*SS***, and **3**. This material is available free of change via Internet at http://pubs.acs.org.

AUTHOR INFORMATION

Corresponding Author

*T.H.: address, Faculty of Education, Shimane University, 1060 Nishikawatsu-Cho, Matsue, Shimane 690-0854, Japan; tel, +81-852-32-9870; fax, +81-852-32-9870; e-mail, h-takashi@edu.shimane-u.ac.jp. T.K.: address, Graduate School of Materials Science, Nara Institute of Science and Technology, 8916-5, Takayama-Cho, Ikoma, Nara 630-0192, Japan; tel, +81-743-72-6170; fax, +81-743-72-6170; e-mail, tkawai@ms.naist.jp.

Notes

The authors declare no competing financial interest.

■ ACKNOWLEDGMENTS

A part of this work was supported by a Grant-in-Aid for Scientific Research on an Innovative Area "Coordination Programming" (no. 2107) from the Ministry of Education, Culture, Sports, Science and Technology, MEXT, Japan. The authors thank Mr. S. Katao and Y. Okajima, technical staff at Nara Institute of Science and Technology (NAIST) for single crystal X-ray analyses and emission decay measurements. This paper was improved through the suggestions and comments of Professor Leigh McDowell (Nara Institute of Science and Technology).

■ REFERENCES

(1) (a) Aspinall, H. C. *Chem. Rev.* **2002**, *102*, 1807−1850. (b) Shibasaki, M.; Kanai, M.; Matsunaga, S.; Kumagai, N. *Acc. Chem. Res.* **2009**, *42*, 1117−1127. (c) Noyori, R. *Asymmetric Catalysis in Organic Synthesis*; John Wiley & Sons: New York, 1994.

(2) (a) Riehl, J. P.; Richardson, F. S. *J. Chem. Phys.* **1976**, *65*, 1011−1021. (b) Richardson, F. S.; Riehl, J. P. *Chem. Rev.* **1977**, *77*, 773−792. (c) Richardson, F. S. *Inorg. Chem.* **1980**, *19*, 2806−2812. (d) Reid, M. F.; Richardson, F. S. *Chem. Phys. Lett.* **1983**, *95*, 501−506. (e) Riehl, J. P.; Richardson, F. S. *Chem. Rev.* **1986**, *86*, 1−16. (f) Parker, D.; Dickins, R. S.; Puschmann, H.; Crossland, C.; Howard, J. A. K. *Chem. Rev.* **2002**, *102*, 1977−2010. (g) Riehl, J. P.; Muller, G. Circulaly Polarized Luminescence Spectroscopy from Lanthanide Systems. In *Handbook on the Physics and Chemistry of Rare Earths*; Gschneidner, K. A., Bünzli, J.-C. G., Pechcharsky, V. K., Eds.; North Holland Publishing Company: Amsterdam, 2005, Vol. *34*; pp 289−357. (h) dos Santos, C. M. G.; Harte, A. J.; Quinn, S. J.; Gunnlaugsson, T. *Coord. Chem. Rev.* **2008**, *252*, 2512−2527. (i) Muller, G. *Dalton Trans.* **2009**, *44*, 9692−9707.

(3) (a) Blok, P. M. L.; Dekkers, H. P. J. M. *Chem. Phys. Lett.* **1989**, *161*, 188−194. (b) Phillips, K. E. S.; Katz, T. J.; Jockusch, S.; Lovinger, A. J.; Turro, N. J. *J. Am. Chem. Soc.* **2001**, *123*, 11899−11907. (c) Goto, H.; Akagi, K. *Angew. Chem., Int. Ed.* **2005**, *44*, 4322−4328. (d) Satrijo, A.; Meskers, S. C. J.; Swager, T. M. *J. Am. Chem. Soc.* **2006**, *128*, 9030−9031. (e) Kawai, T.; Kawamura, K.; Tsumatori, H.; Ishikawa, M.; Naito, M.; Fujiki, M.; Nakashima, T. *ChemPhysChem* **2007**, *8*, 1465−1468. (f) Tsumatori, H.; Nakashima, T.; Kawai, T. *Org. Lett.* **2010**, *12*, 2362−2365. (g) Kaseyama, T.; Furumi, S.; Zhang, X.; Tanaka, K.; Takeuchi, M. *Angew. Chem., Int. Ed.* **2011**, *50*, 3684−3687. (h) Tsubomura, T.; Morishita, S.; Andoh, H.; Morita, M. *Inorg. Chem.* **1995**, *34*, 5094−5096. (i) Gunde, K. E.; Credi, A.; Jandrasics, E.; von Zelewski, A.; Richardson, F. S. *Inorg. Chem.* **1997**, *36*, 426−434. (j) Schaffner-Hamann, C.; von Zelewskey, A.; Barbieri, A.; Barigelletti, F.; Muller, G.; Riehl, J. P.; Neels, A. *J. Am. Chem. Soc.* **2004**, *126*, 9339−9348. (k) Oyler, K. D.; Coughlin, F. J.; Bernhard, S. *J. Am. Chem. Soc.* **2007**, *129*, 210−217. (l) Coughlin, F. J.; Westrol, M. S.; Oyler, K. D.; Byrne, N.; Kraml, C.; Zysman-Colman, E.; Lowry, M. S.; Bernhard, S. *Inorg. Chem.* **2008**, *47*, 2039−2048. (m) Ashizawa, M.; Yang, L.; Kobayashi, K.; Sato, H.; Yamagishi, A.; Okuda, F.; Harada, T.; Kuroda, R.; Haga, M. *Dalton Trans.* **2009**, *10*, 1700−1702. (n) Yang, L.; von Zelewski, A.; Nguyen, H. P.; Muller, G.; Labat, G.; Stoeckli-Evans, H. *Inorg. Chim. Acta* **2009**, *362*, 3853−3856.

(4) (a) Petoud, S.; Muller, G.; Moore, E. G.; Xu, J.; Sokolnicki, J.; Riehl, J. P.; Le, U. N.; Cohen, S. M.; Raymond, K. N. *J. Am. Chem. Soc.* **2007**, *129*, 77−83. (b) Leonard, J. P.; Jensen, P.; McCabe, T.; O'Brien, J. E.; Peacock, R. D.; Kruger, P. E.; Gunnlaugsson, T. *J. Am. Chem. Soc.* **2007**, *129*, 10986−10987. (c) Seitz, M.; Moore, E. G.; Ingram, A. J.; Muller, G.; Raymond, K. N. *J. Am. Chem. Soc.* **2007**, *129*, 15468−15470. (d) Seitz, M.; Do, K.; Ingram, A. J.; Moore, E. G.; Muller, G.; Raymond, K. N. *Inorg. Chem.* **2009**, *48*, 8469−8479. (e) Stomeo, F.; Lincheneau, C.; Leonard., J. P.; O'Brien, J. E.; Peacock, R. D.; McCoy, C. P.; Guunlaugsson, T. *J. Am. Chem. Soc.* **2009**, *131*, 9396−9397. (f) Samuel, A. P. S.; Lunkley, J. L.; Muller, G.; Raymond, K. N. *Eur. J. Inorg. Chem.* **2010**, *21*, 3343−3347.

(5) (a) Peeters, E.; Christiaans, M. P. T.; Janssen, R. A. J.; Schoo, H. F. M.; Dekkers, H. P. J. M.; Meijer, E. W. *J. Am. Chem. Soc.* **1997**, *119*, 9909−9910. (b) Yu, J.; Parker, D.; Pal, R.; Poole, R. A.; Cann, M. J. *J. Am. Chem. Soc.* **2006**, *128*, 2294−2299. (c) Montgomery, C. P.; New, E. J.; Parker, D.; Peacock, R. D. *Chem. Commun.* **2008**, *36*, 4261−4263. (d) Moussa, A.; Pham, C.; Bommireddy, S.; Muller, G. *Chirality* **2009**, *21*, 497−506. (e) Maeda, H.; Bando, Y.; Shimomura, K.; Yamada, I.; Naito, M.; Nobusawa, K.; Tsumatori, H.; Kawai, T. *J. Am. Chem. Soc.* **2011**, *133*, 9266−9269.

(6) (a) Werts, M. H. V.; Jukes, R. T. F.; Verhoeven, J. W. *Phys. Chem. Chem. Phys.* **2002**, *4*, 1542−1548. (b) Beeby, A.; Clarkson, I. M.; Dickins, R. S.; Faulkner, S.; Parker, D.; Royle, L.; de Sousa, A. S.; Williams, J. A. G.; Woods, M. *J. Chem. Soc., Perkin Trans 2* **1999**, *3*, 493−503.

(7) (a) Berry, M. T.; Reid, M. F.; Richardson, F. S. *J. Chem. Phys.* **1986**, *84*, 2917−2925. (b) Richardson, F. S.; Berry, M. T.; Reid, M. F. *Mol. Phys.* **1986**, *58*, 929−945.

(8) (a) Sastri, V. S.; Perumareddi, J. R.; Rao, V. R.; Rayudu, G. V. S.; Bünzli, J.-C. G. Structural Chemistry of Lanthanide Complexes. In *Modern Aspects of Rare Earths and Their Complexes*; Elsevier Science Publishing: Amsterdam, 2003; Chapter 5, pp 375−422. (b) Orgen, J. S. *Introduction to Molecular Symmetry*; Evans, J., Ed.; Oxford University Press: New York, 2001.

(9) (a) Gregoliński, J.; Lisowski, J. *Angew. Chem., Int. Ed.* **2006**, *45*, 6122−6126. (b) Gregoliński, J.; Starynowicz, P.; Hua, K. T.; Lunkley, J. L.; Muller, G.; Lisowski, J. *J. Am. Chem. Soc.* **2008**, *130*, 17761−17773. (c) Harada, T.; Nakano, Y.; Fujiki, M.; Naito, N.; Kawai, T.; Hasegawa, Y. *Inorg. Chem.* **2009**, *48*, 11242−11250.

(10) (a) Lama, M.; Mamula, O.; Kottas, G. S.; Rizzo, F.; De Cola, L.; Nakamura, A.; Kuroda, R.; Stoeckli-Evans, H. *Chem.—Eur. J.* **2007**, *13*, 7358−7373. (b) Lama, M.; Mamula, O.; Kottas, G. S.; De Cola, L.; Stoeckli-Evans, H.; Shova, S. *Inorg. Chem.* **2008**, *47*, 8000−8015.

(11) Yuasa, J.; Ohno, T.; Miyata, K.; Tsumatori, H.; Hasegawa, Y.; Kawai, T. *J. Am. Chem. Soc.* **2011**, *133*, 9892−9902.

(12) (a) Matsumoto, K.; Suzuki, K.; Tsukuda, T.; Tsubomura, T. *Inorg. Chem.* **2010**, *49*, 4717−4719. (b) Stanley, J. M.; Zhu, X.; Yang, X.; Holliday, B. J. *Inorg. Chem.* **2010**, *49*, 2035−2037. (c) Desimoni, G.; Faita, G.; Quadrelli, P. *Chem. Rev.* **2003**, *103*, 3119−3154.

(13) (a) Brittain, H. G.; Richardson, F. S. *J. Am. Chem. Soc.* **1976**, *98*, 5858−5863. (b) Brittain, H. G. *Inorg. Chem.* **1980**, *19*, 2233−2236. (c) Schippers, P. H.; van den Beukel, A.; Dekkers, H. P. J. M. *J. Phys. E: Sci. Instr.* **1982**, *15*, 945−950.

(14) (a) Shirotani, D.; Suzuki, T.; Kaizaki, S. *Inorg. Chem.* **2006**, *45*, 6111−6113. (b) Lunkley, J. L.; Shirotani, D.; Yamanari, K.; Kaizaki, S.; Muller, G. *J. Am. Chem. Soc.* **2008**, *130*, 13814−13815. (c) Shirotani, D.; Suzuki, T.; Yamanari, K.; Kaizaki, S. *J. Alloys Compd.* **2008**, *451*, 325−328. (d) Sato, H.; Shirotani, D.; Yamanari, K.; Kaizaki, S. *Inorg. Chem.* **2010**, *49*, 356−358.

(15) Eliseeva, S. V.; Kotova, O. V.; Gumy, F.; Semenov, S. N.; Kessler, V. G.; Lepnev, L. S.; Bünzli, J.-C. G.; Kuzmina, N. P. *J. Phys. Chem. A* **2008**, *112*, 3614−3626.

(16) Xu, J.; Radkov, E.; Ziegler, M.; Raymond, K. N. *Inorg. Chem.* **2000**, *39*, 4156−4164.

(17) (a) Kepert, D. L. Aspects of the Stereochemistry of Six-Coordination. In *Progress in Inorganic Chemistry*; Lippard, S. J., Ed; Wiley: NJ, 1977; Chapter 23, pp 179−249. (b) Kepert, D. L. Aspects of the Stereochemistry of Eight-Coordination. In *Progress in Inorganic Chemistry*; Lippard, S. J., Ed; Wiley: NJ, 1978; Chapter 24, pp 1−65.

(18) Desiraju, G. R.; Steiner, T. *The Weak Hydrogen Bond in Structural Chemistry and Biology*; Oxford University Press: Oxford, 1999.

(19) (a) Boucher, L. J. *Inorg. Chem.* **1970**, *9*, 1202−1207. (b) Zahn, S.; Canary, J. W. *Angew. Chem., Int. Ed.* **1998**, *37*, 305−307.

(20) (a) Tsukube, H.; Shinoda, S. *Chem. Rev.* **2002**, *102*, 2389−2403. (b) Subhan, M. A.; Hasegawa, Y.; Suzuki, T.; Kaizaki, S.; Yanagida, S. *Inorg. Chim. Acta* **2009**, *362*, 136−142.

(21) (a) Hasegawa, Y.; Yamamuro, M.; Wada, Y.; Kanehisa, N.; Kai, Y.; Yanagida, S. *J. Phys. Chem. A* **2003**, *107*, 1697−1702. (b) Nakamura, K.; Hasegawa, Y.; Kawai, H.; Yasuda, N.; Kanehisa, N.; Kai, Y.;

Nagamura, T.; Yanagida, S.; Wada, Y. *J. Phys. Chem. A* **2007**, *111*, 3029−3037. (c) Miyata, K.; Hasegawa, Y.; Kuramochi, Y.; Nakagawa, T.; Yokoo, T.; Kawai, T. *Eur. J. Inorg. Chem.* **2009**, *32*, 4777−4785. (d) Moudam, O.; Rowan, B. C.; Alamiry, M.; Richardson, P.; Richards, B. S.; Jones, A. C.; Robertson, N. *Chem. Commun.* **2009**, *43*, 6649−6651. (e) Miyata, K.; Nakagawa, T.; Kawakami, R.; Kita, Y.; Sugimoto, K.; Nakashima, T.; Harada, T.; Kawai, T.; Hasegawa, Y. *Chem.—Eur. J.* **2011**, *17*, 521−528.

(22) (a) Judd, B. R. *Phys. Rev.* **1962**, *127*, 750−761. (b) Ofelt, G. S. *J. Chem. Phys.* **1962**, *37*, 511−520.

(23) (a) New., E. J.; Parker, D.; Peacock, R. D. *Dalton Trans.* **2009**, *28* (4), 672−679. (b) Lincheneau, C.; Destribats, C.; Barry, D. E.; Kitchen, J. A.; Peacock, R. D.; Gunnlaugsson, T. *Dalton Trans.* **2011**, *40*, 12056−12059. (c) Kitchen, J. A.; Barry, D. E.; Mercs, L.; Albrecht, M.; Peacock, R. D.; Guunlaugsson, T. *Angew. Chem., Int. Ed.* **2012**, *124*, 728−732.

(24) Porcher, P.; Caro, P. *J. Lumin.* **1980**, *21*, 207−216.

(25) (a) Dieke, G. H. *Spectra and Energy Lebels of Rare Earth Ions in Crystals*; Crosswhite, H. M., Crosswhite, H., Eds.; Wiley Interscience: New York, 1968. (b) Stein, G.; Würzberg, E. *J. Chem. Phys.* **1975**, *62*, 208−213. (c) Wegh, R.; Meijerrink, A.; Lamminmäki, R.-J.; Hölsä, J. *J. Lumin.* **2000**, *87*−*89*, 1002−1004.

(26) (a) Hasegawa, Y.; Kimura, Y.; Murakoshi, Y.; Wada, Y.; Kim, J.-H.; Nakashima, N.; Yamanaka, T.; Yanagida, S. *J. Phys. Chem.* **1996**, *100*, 10201−10205. (b) Hasegawa, Y.; Ohkubo, T.; Sogabe, K.; Kawamura, Y.; Wada, Y.; Nakashima, N.; Yanagida, S. *Angew. Chem., Int. Ed.* **2000**, *39*, 357−360. (c) Mancino, G.; Ferguson, A. J.; Beeby, A.; Long, N. J.; Jones, T. S. *J. Am. Chem. Soc.* **2005**, *127*, 524−525. (d) Harada, T.; Hasegawa, Y.; Nakano, Y.; Fujiki, M.; Naito, M.; Wada, T.; Inoue, Y.; Kawai, T. *J. Alloys Compd.* **2009**, *488*, 599−602. (e) Kishimoto, S.; Nakagawa, T.; Kawai, T.; Hasegawa, Y. *Bull. Chem. Soc. Jpn.* **2011**, *84*, 148−154.

(27) (a) Bünzli, J.-C. G.; Chauvin, A.-S.; Kim, H. K.; Deiters, E.; Eliseeva, S. V. *Coord. Chem. Rev.* **2010**, *254*, 2623−2633. (b) Shavaleev., N. M.; Eliseeva, S. V.; Scopelliti, R.; Bünzli, J.-C. G. *Inorg. Chem.* **2010**, *49*, 3927−3936.